Theoretical and Experimental Studies of Indoaniline Dyes. A Novel Relationship between Absorption Spectra and Molecular Structure

Masafumi Adachi, Yukichi Murata, and Shinichiro Nakamura*

Contribution from the Mitsubishi Kasei Corporation, Research Center, 1000 Kamoshida-cho, Midori-ku, Yokohama 227, Japan

Received September 25, 1992

Abstract: The longest absorption band of indoaniline dyes depends on the dihedral angle between the quinone and the aniline rings. The absorption shifts to longer wavelength and the absorption intensity decreases upon increasing the dihedral angle (18° → 90°) with the loss of planarity. This wavelength change is not consistent with the generally accepted concept that the more planar the molecule, the larger the red shift because of the increased π-conjugation. The novel spectrum change has been examined by INDO/S and AM1 methods on the basis of experimental results. The change cannot be explained by the HOMO–LUMO energy gap. The configuration interaction plays an essential role, and the imino N atom lone pair to LUMO transition is especially involved. The relationship between the absorption spectrum and the structure has been obtained. This reproduces well the observed spectra and X-ray structure of indoaniline dyes. The detailed features of the dihedral angle dependent wavelength shift have been discussed focusing on the essential role of configuration mixing induced by the structural change. On the basis of these findings, the altering of the dihedral angle for the tuning of the absorption spectrum can be achieved by adjusting substituents, such as the introduction of a bulky substituent or an intramolecular hydrogen bond. The current analysis extends the existing concept for long wavelength absorption (by large π–conjugation) and provides a new guiding principle for the design of functional dyes. The principle is not limited to the present series of dyes but can be applicable to a wide range of dyes having a nonplanar structure.

1. Introduction

Indoaniline dyes are widely used cyan color dyes. Their applications include photography,[1] D2T2 system,[2] and other various colored materials, where the absorption spectrum design is of crucial importance. However, the guiding principle of the molecular design of indoaniline dye has not yet been well established. A generally accepted concept, for the relationship between structure and absorption spectrum, requires the maximum planarity for producing the red shift because of the increase of π-conjugation. Syntheses based on this principle have not provided indoaniline dyes with the expected properties. The generally accepted guiding principle is not effective for this class of dyes. Therefore, a study to explain why the conventional concept is not applicable and a study to provide a new concept are in order. This problem has motivated us to analyze the spectra of various indoaniline dyes by using the molecular orbital method and to obtain a guiding principle for the rational design of new indoaniline dyes.

The investigation of indoaniline dyes was pioneered, about 50 years ago, by Vittum, Brown, and collaborators. They reported the substituent effect of indoaniline dyes systematically.[3] Issa et al. also reported substituent effects, including the subabsorption bands.[4] Figueras reported the absorption spectra of phenol blue and derivatives focusing on the hydrogen bond and solvent effect.[5] Panchártek presented the substituent effect of the quinone ring.[6] On the indoaniline dyes the relationship between electrochemical redox potentials and the longest absorption wavelength was studied by Stradins et al.[7] Theoretical analyses of HMO and ASMO CI by Smith et al. for indoaniline dye also appeared,[8] the results included the qualitative substituent effect. The determination of molecular structure of azomethine dyes (including phenol blue) by CNDO/2 and their absorption spectra by PPP-CI were presented by Hofmann et al.;[9] they showed that those dyes were not planar. Recently Yue et al.[10] showed the substituent effect for absorption wavelength by PPP-CI; however, no correlations with the observed intensities were mentioned.

No clear explanation of the spectrum–structure relationship for indoaniline dyes has been previously given. Molecules, having an azomethine bridge, 2',6'-disubstituted in the aniline ring[8,11] or 3,5-disubstituted in the quinone ring[3b] were commonly reported as typical examples of dyes with long wavelength absorption and small extinction coefficients. These effects were explained by invoking steric hindrance. Why steric hindrance could produce the red shift and the weak absorption was not at all clear. Many previous researchers experimenting with indoaniline dyes[3,8,10] did not consider nonplanarity of the quinone and aniline rings, most probably because of insufficient experimental data, and because the early analyses were done by the PPP method which was suitable for planar π-conjugated molecules. Now X-ray structure analysis data have been extensively accumulated.[12] These data have

(1) Nickel, U. *J. Imag. Tech.* **1986**, *12*, 181.
(2) Niwa, T.; Murata, Y.; Maeda, S. (Mitsubishi Chem. Ind. Ltd.) DE 3,524,519. Apr 7, 1988.
(3) (a) Vittum, P. W.; Brown, G. H. *J. Am. Chem. Soc.* **1946**, *68*, 2235. (b) Vittum, P. W.; Brown, G. H. *J. Am. Chem. Soc.* **1947**, *69*, 152. (c) Vittum, P. W.; Brown, G. H. *J. Am. Chem. Soc.* **1949**, *71*, 2287. (d) Barr, C. R.; Brown, G. H.; Thirtle, J. R.; Weissberger, A. *Photograph. Sci. Eng.* **1961**, *5*, 195. (e) Lurie, A. P.; Brown, G. H.; Thirtle, J. R.; Weissberger, A. *J. Am. Chem. Soc.* **1961**, *83*, 5015.
(4) (a) Issa, I. M.; El-Shafei, A. K.; Etaiw, S. H.; El-Kashef, H. S. *J. F. Prakt. Chem.* **1978**, *320*, 557. (b) Issa, I. M.; El Samahy, A. A.; Issa, R. M.; El Kasher, H. S. *Rev. Roum. Chim.* **1978**, *23*, 617.
(5) Figueras, J. *J. Am. Chem. Soc.* **1971**, *93*, 3255.
(6) Panchártek, J. *Sb. Prednasek-Symp. Fotochem., Fotofyz. Ved. Fotogr.: Acad. Mezinar. Ucasti, 6th*; Vys. Sk. Chem.-Technol.: Pardubice, Czechoslovakia, 1977; p 244.
(7) (a) Glezer, V.; Medina, B.; Stradins, J.; Freimanis, J.; Markava, E. *Latv. PSR Zinat. Akad. Vestis, Kim. Ser.* **1986**, 229. (b) Stradiņš, J.; Glezer, V.; Turovska, B.; Markava, E.; Freimanis, J. *Electrochim. Acta* **1991**, *36*, 1219.
(8) Smith, W. F., Jr. *Terahedron* **1964**, *20*, 671.
(9) Hofmann, H.-J.; Höppner, F.-D.; Weiss, C. *J. Signalaufzeichnungsmaterialien* **1974**, *2*, 97.
(10) Yue, C.; Zhen-hua, Z.; Zu-guang, Y.; Su-ying, W. *Ganguang Kexue Yu Kuang Huaxue* **1986**, 7.
(11) Rieker, A.; Kessler, H. *Z. Naturforsch. B: Anorg. Chem., Org. Chem., Biochem., Biophys., Biol.* **1966**, *21*, 939.

0002-7863/93/1515-4331$04.00/0

revealed that the azomethine bridged molecules are not planar. Since the indoaniline dye is a nonplanar molecule, all valence bond electrons (σ and π electron) must be considered in the calculation. Therefore, we have chosen the INDO/S method[13] for the absorption spectrum study (together with the AM1 method[14] for determination of the molecular structure). We have already reported the validity of the INDO/S method for analyses of dye absorption spectrum.[15] Moreover, in the analysis of structure–absorption relationship in near-infrared absorbing dyes of the naphthoquinone methide type, the INDO/S calculations have proven to be reliable.[16]

In this paper, we present the relationship of the structure and the absorption spectrum of the indoaniline dye which is the most representative azomethine dye, on the basis of the observed and the calculated absorption spectrum (wavelength and oscillator strength). The results are surprisingly not consistent with the conventional concept, quite the opposite; the less the planarity, the longer is the absorption wavelength. The origin of this effect has been investigated through a detailed study of the electronic structures. In addition to the main transition, the second and third transition character of indoaniline dyes has also been analyzed. Moreover, by using the obtained relationship, we have demonstrated a dye design (tuning the λ_{max} and the absorption intensity) by adjusting the substituents (for example bulkiness or intramolecular hydrogen bond). The current study suggests a new guiding principle for the design of indoaniline dyes. Reflecting the nature of the discussion developed in this study and our previous study,[16] the principle thus obtained can be a general one, which is not limited to indoaniline dyes.

2. Experimental Section

Spectroscopic Measurements. The dyes were dissolved in Junsei Chemical Co. Ltd. spectrum grade solvents to give 2×10^{-5} M solutions which were read in 1-cm cells with the Hitachi Automatic Recording Spectrophotometer (U-3400).

Preparation and Identification of Dyes. Dyes **1–4** were prepared by oxidative condensation of suitable *p*-phenylenediamines and phenols using ammonium persulfate as oxidant, following the procedure of Vittum and Brown.[3a] All dyes were purified by column chromatography giving one spot on a thin-layer chromatographic plate.

Dye identification was carried out by the usual methods. Melting points were uncorrected.

***N*-[3-[[4-(Diethylamino)phenyl]imino]-6-oxo-1,4-cyclohexadien-1-yl]-acetamide (1)**: mp 127–128 °C; mass spectrum, *m/e* 311 (M^+), 296 ($M^+ - CH_3$). Anal. Calcd for $C_{18}H_{21}N_3O_2$: C, 69.43; H, 6.80; N, 13.49. Found: C, 69.23; H, 6.95; N, 13.46.

***N*-[3-[[2-Methyl-4-(diethylamino)phenyl]imino]-6-oxo-1,4-cyclohexadien-1-yl]acetamide (2)**: mp 229–230 °C; mass spectrum, *m/e* 325 (M^+), 310 ($M^+ - CH_3$). Anal. Calcd for $C_{19}H_{23}N_3O_2$: C, 70.13; H, 7.12; N, 12.91. Found: C, 70.05; H, 7.33; N, 13.00.

***N*-[3-[[2,6-Dimethyl-4-(diethylamino)phenyl]imino]-6-oxo-1,4-cyclohexadien-1-yl]acetamide (3)**: mp 149–150 °C; mass spectrum, *m/e* 339 (M^+), 324 ($M^+ - CH_3$). Anal. Calcd for $C_{20}H_{25}N_3O_2$: C, 70.77; H, 7.42; N, 12.38. Found: C, 70.51; H, 7.25; N, 12.18.

***N*-[3-[[2-(Acetylamino)-4-(diethylamino)phenyl]imino]-6-oxo-1,4-cyclohexadien-1-yl]acetamide (4)**: mp 184–185 °C; mass spectrum, *m/e* 368 (M^+), 353 ($M^+ - CH_3$). Anal. Calcd for $C_{20}H_{24}N_4O_3$: C, 65.20; H, 6.57; N, 15.21. Found: C, 64.96; H, 6.50; N, 14.91.

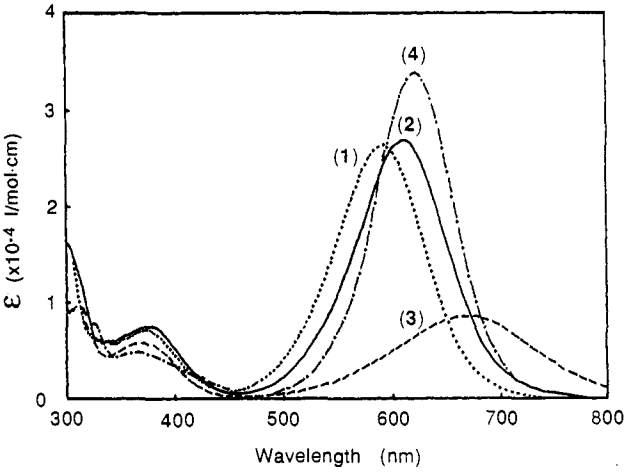

Figure 1. Absorption spectra of indoaniline dyes (in cyclohexane solution).

3. Calculations

Calculations were performed by the INDO/S method (modified for spectral calculations).[13] The electronic repulsion integral was evaluated by the Nishimoto-Mataga formula.[17] All SCF calculations were executed at the closed shell Hartree–Fock level (RHF). Configuration interaction (CI) calculations included single excited configurations from the ground state, consisting of 14 (occupied) × 14 (virtual) configurations.

The molecular geometries of indoaniline dyes **1**, **2**, **3**, and **4** were generated on the basis of the X-ray structures for **2**.[18] For **1** the hydrogen atom was substituted by the standard bond length,[19] for **2** X-ray data were directly adopted,[18] for **3** the added CH_3 structure was optimized by AM1 method,[14] and for **4** the added $NHCOCH_3$ structure was taken from the naphthoquinone methide dye X-ray structure[12f] with partial optimization by the AM1 method. The dihedral angle of the quinone and the aniline rings for every molecule was optimized by the AM1 method by fixing the other geometrical parameters.

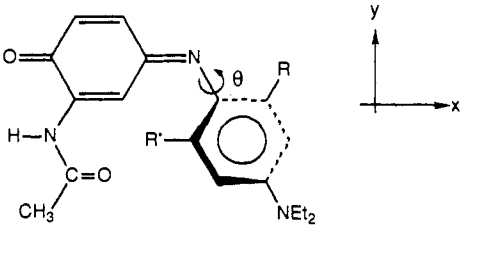

(1) R=H, R'=H
(2) R=CH_3, R'=H
(3) R=CH_3, R'=CH_3
(4) R=$NHCOCH_3$, R'=H

4. Results and Discussion

A. Relation of the Dihedral Angle and the Absorption Property. The observed absorption spectra of indoaniline dyes **1–4** are shown in Figure 1. In Table I, the absorption wavelength and intensity

(12) (a) Fraterman, H. A.; Romers, C. *Recl. Trav. Chim. Pays-Bas* **1971**, *90*, 364. (b) Poveteva, Z. P.; Chetkina, L. A.; Kopilov, V. V. *Zh. Strukt. Khim.* **1980**, *21*, 118. (c) Klerks, J. M.; Van Koten, G.; Vrieze, K. *J. Organomet. Chem.* **1981**, *219*, 9. (d) Rychlewska, U.; Broom, M. B. H.; Eggleston, D. S.; Hodgson, D. J. *J. Am. Chem. Soc.* **1985**, *107*, 4768. (e) Alberti, A.; Grecim, L.; Stipa, P.; Sgarabotto, P.; Ugozzoli, F. *Tetrahedron* **1987**, *43*, 3031. (f) Kubo, Y.; Kuwana, M.; Yoshida, K.; Tomotake, Y.; Matsuzaki, T.; Maeda, S. *J. Chem. Soc., Chem. Commun.* **1989**, 35. (g) Deadman, J. J.; Jarman, M.; McCague, R.; McKenna, R.; Neidle, S. *J. Chem. Soc., Perkin Trans. II* **1989**, 971. (h) Chi, K.-M.; Calabrese, J. C.; Milller, J. S. *Mol. Cryst. Liq. Cryst.* **1989**, *176*, 173. (i) Carloni, P. C.; Greci, L.; Stipa, P.; Alberti, A.; Rizzoli, C.; Sagarabotto, P.; Ugozzoli, F. *J. Chem. Soc., Perkin Trans. 2* **1990**, 185.

(13) (a) Ridley, J. E.; Zerner, M. C. *Theor. Chim. Acta* **1973**, *32*, 111. (b) Bacon, A. D.; Zerner, M. C. *Theor. Chim. Acta* **1979**, *53*, 21. (c) Zerner, M. C.; Loew, G. H.; Kirchner, R. F.; Mueller-Westerhoff, U. T. *J. Am. Chem. Soc.* **1980**, *102*, 589.

(14) (a) Dewar, M. J. S.; Zoebisch, E. G.; Healy, E. F.; Stewart, J. J. P. *J. Am. Chem. Soc.* **1985**, *107*, 3902. (b) MOPAC Ver. 5, Stewart, J. J. P. *QCPE Bull.* **1989**, *9*, 10.

(15) Adachi, M.; Nakamura, S. *Dyes Pig.* **1991**, *17*, 287.

(16) Kubo, Y.; Yoshida, K.; Adachi, M.; Nakamura, S.; Maeda, S. *J. Am. Chem. Soc.* **1991**, *113*, 2868.

(17) (a) Nishimoto, K.; Mataga, N. *Z. Phys. Chem.* (*Frankfurt am Main*) **1957**, *12*, 335. (b) Mataga, N.; Nishimoto, K. *Z. Phys. Chem.* (*Frankfurt am Main*) **1957**, *13*, 140.

(18) Osano, Y. T.; Matsuzaki, T.; Murata, Y., manuscript in preparation.

Table I. Observed and Calculated Absorption Spectra of Indoaniline Dyes

dye	R	R′	obsd[a] λ_{max} (nm)	obsd[a] ϵ (1/mol·cm)	dihedral angle[b] (deg)	calcd (INDO/S) λ_{max} (nm)	calcd (INDO/S) f[c]
1	H	H	590	26500	47.1	508.7	0.413
						450.3	0.004
			373	7200		351.0	0.272
2	CH_3	H	609	27000	46.7[d]	514.9	0.432
						448.7	0.003
			378	7600		351.4	0.313
3	CH_3	CH_3	666	8400	68.3[e]	562.5	0.116
						449.6	0.002
			369	5700		348.8	0.278
4	$NHCOCH_3$	H	622	34100	42.0	524.9	0.536
						451.0	0.003
			363	4800		353.3	0.230

[a] Cyclohexane solution (10^{-4}–10^{-5} mol/L). [b] Optimized by AM1 method. [c] Oscillator strength. [d] X-ray value is 44.5°. [e] X-ray value is 56.7°.

of the longest and the next absorption band are shown together with the calculated values at the optimum dihedral angle of the quinone and the aniline rings. The calculated dihedral angle 46.7° in **2** reproduces well the X-ray value of 44.5°. This assures the validity of geometries for the molecules whose X-ray data are not available. Moreover, as an additional conformation, Table II shows the calculated absorption spectrum of **2** at the X-ray structure[18] with the assignments of transition character.

(i) The First Transition (the Longest Absorption Band, S_1 State). Comparing the observed and the calculated absorption spectra (Table I) of **2** and **3**, the longer λ_{max} is obtained for **3** than for **2** in spite of a larger dihedral angle for **3** that implies less planarity and less π-conjugation. The result is a typical example of the novel relationship of the dihedral angle and the absorption properties for indoaniline dyes. In an attempt to shed light on the mechanism, we have examined the relationship of the dihedral angle (of the quinone and the aniline rings) to the λ_{max} and the oscillator strength for the dye **2**. The results are shown in Table III and Figure 2.[20] Increasing the dihedral angle (18° → 90°), the λ_{max} extends to longer wavelengths, while the oscillator strength decreases. Indeed, the λ_{max} change is not consistent with a general concept. At the angle of 90°, the longest λ_{max} and the smallest (almost zero) oscillator strength are obtained. The longest absorption band consists of a mainly HOMO, localized in the aniline ring, to LUMO, localized in the quinone ring, (Figure 3) charge transfer (CT) type transition (Table II).

The decrease of the oscillator strength can be explained by the decrease of the overlap of the wave function of ground and excited states. However, the λ_{max} change turns out to be less simple. Usually a λ_{max} change can be explained by a HOMO and/or LUMO energy level change. The HOMO–LUMO energy gap ($\Delta\epsilon_{HOMO,LUMO}$) as a function of the dihedral angle, shown in Figure 4, does not decrease upon increasing the dihedral angle. Thus the λ_{max} change cannot be explained by the HOMO–LUMO energy gap.

(ii) Analysis of the Dihedral Angle Dependence of the Longest Absorption Band. We have examined the reason for the λ_{max} change by analyzing the electronic state. The excitation energy ΔE within the HF level, which is a more precise estimation than by the HOMO–LUMO gap $\Delta\epsilon$, has been calculated. The HOMO → LUMO excitation energy ($\Delta\epsilon_{HOMO\rightarrow LUMO}$) is expressed by using electronic interaction terms J and K

(19) *Tables of Interatomic Distances and Configuration in Molecules and Ions, The Chemical Society Special Publication, No. 11, 18*; Sutton, L. E. Ed.; The Chemical Society: London, 1958, 1965.

(20) In figures, small dihedral angle region (0–18°) is not shown, because the calculated results are suffering from the unusual small distance of the quinone 3 position H atom and the aniline 6′ position H atom.

Table II. Transition Character of Dye (**2**)

obsd[a] λ_{max} (nm)	obsd[a] ϵ (1/mol·cm)	calcd (INDO/S)[b] λ_{max} (nm)	f[d]	transition character[c]
609	27000	512.3	0.467	−0.884{(HOMO,63) → (LUMO,64)}
		448.7	0.003	−0.722{(58) → (64)}
				−0.335{(59) → (64)}
378	7600	352.6	0.324	−0.503{(62) → (64)}
				−0.464{(60) → (64)}
				−0.380{(56) → (64)}
		333.0	0.111	
		325.8	0.034	
		322.8	0.002	

[a] Cyclohexane solution (~10^{-5} mol/L). [b] Calculated at the X-ray structure (dihedral angle 44.5°). [c] Excitations having the CI coefficient over 0.3 are shown. [d] Oscillator strength.

Table III. Calculated First Absorption Band of Dye (**2**) with Transition Character (INDO/S)[a]

dihedral angle (deg)	λ_{max} (nm)	f[c]	transition character[b] HOMO (63) → LUMO (64)	(56) → (64)	(57) → (64)	(59) → (64)
18	476.2	0.786	0.920	0.016	0.196	0.182
29	490.0	0.636	0.894	0.110	0.206	0.238
44.5[d]	512.3	0.467	0.884	0.182	0.131	0.258
58	529.9	0.262	0.882	0.199	0.031	0.278
72	550.2	0.090	0.879	0.200	0.008	*e*
90	566.4	0.004	0.877	0.199	0.006	0.316

[a] See Figures 2 and 9. [b] Absolute value of the CI coefficient. (Excitations having the CI coefficient over 0.2 are shown.) [c] Oscillator strength. [d] X-ray value. [e] The (59)th and the (60)th orbitals are in accidental degeneracy and is not shown.

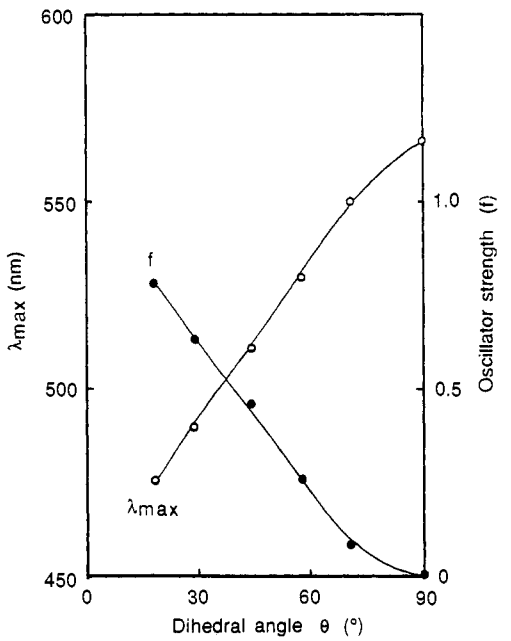

Figure 2. Spectral changes of the first transition of **2** with changes of the dihedral angle of the quinone and the aniline rings (INDO/S).

$$\Delta E_{HOMO\rightarrow LUMO} = \Delta\epsilon_{HOMO,LUMO} - J_{HOMO,LUMO} + 2K_{HOMO,LUMO}$$

($\Delta\epsilon$, HOMO–LUMO gap; J, Coulomb integral; K, exchange integral). The calculated transition energy (the reciprocal value of λ_{max} shown in Figure 2) and the excitation energy changes $\Delta E_{HOMO\rightarrow LUMO}$ with the dihedral angle are shown in Figure 5. When $\Delta E_{HOMO\rightarrow LUMO}$ decreases, the transition energy also decreases as well as the dihedral angle goes from 18° to 90°. Nevertheless, the change of absorption wavelength (noted as S_1 in Figure 5) with the dihedral angle is only partly (about $^1/_3$) covered by the HOMO → LUMO excitation energy change, as

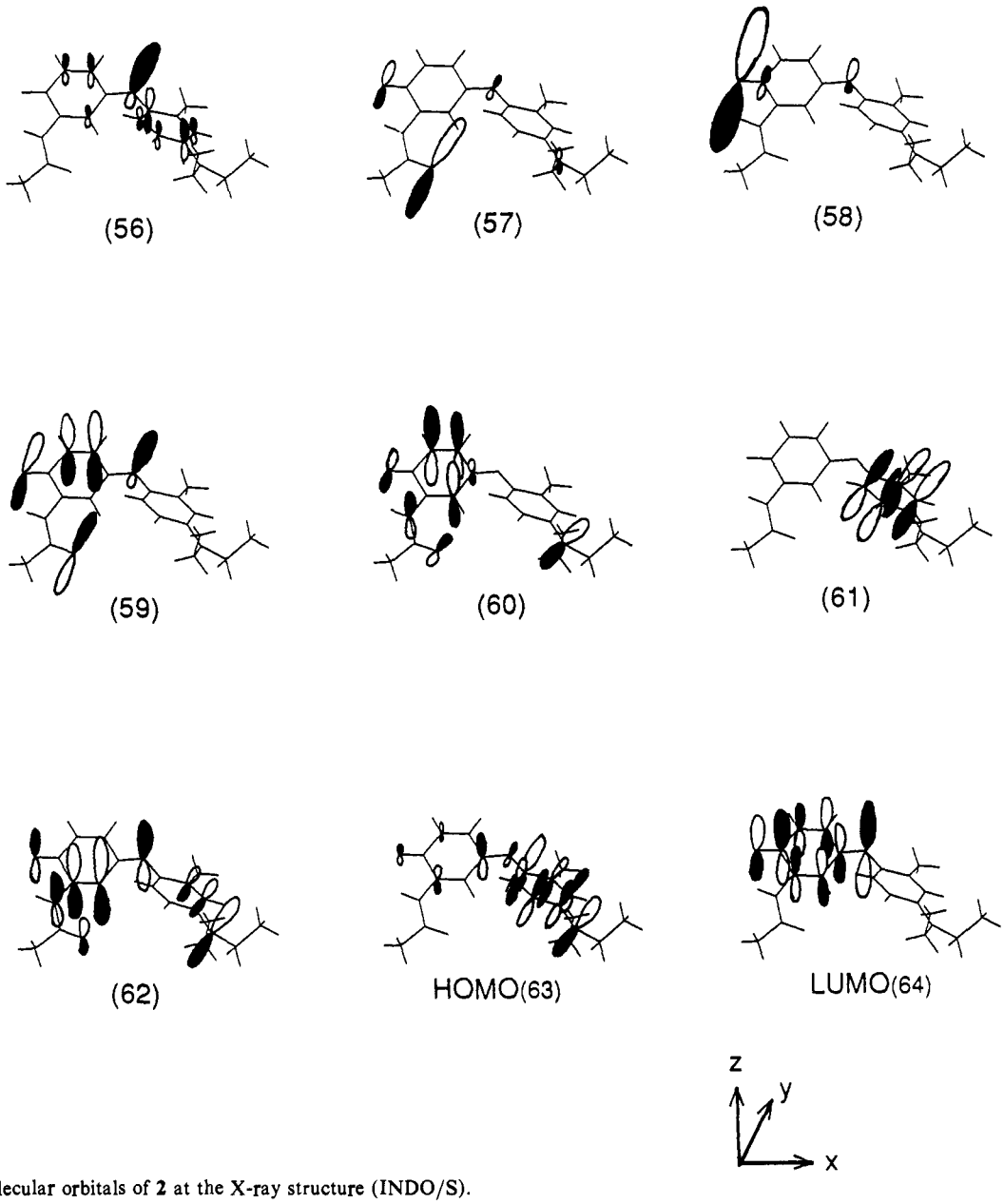

Figure 3. Molecular orbitals of 2 at the X-ray structure (INDO/S).

shown in Figure 5. The details of this $\Delta E_{HOMO\rightarrow LUMO}$ are displayed in Figure 6 by showing each component. Along with the increase of the dihedral angle, $J_{HOMO,LUMO}$ and $2K_{HOMO,LUMO}$ decrease, while $\Delta\epsilon_{HOMO,LUMO}$ is only slightly increased. The decrease of $2K_{HOMO,LUMO}$ is slightly more than $J_{HOMO,LUMO}$. Thus the change of $\Delta E_{HOMO\rightarrow LUMO}$ can be understood as a result of a subtle balance of $J_{HOMO,LUMO}$ and $2K_{HOMO,LUMO}$. The $K_{HOMO,LUMO}$ is zero at 90°, reflecting the complete localization; HOMO only in the aniline ring and LUMO only in the quinone ring (see Figure 7), the overlap of HOMO and LUMO has vanished. In order to visualize the situation shown in Figure 7 (90°), we have displayed the orbitals at the dihedral angle 18° in Figure 8 as a comparison. Obviously HOMO and LUMO localize with increasing the dihedral angle (18° → 90°). The results shown in Figure 6 indicate that the HOMO → LUMO excitation energy change is, in fact, due to only the change of the electronic interaction terms, $J_{HOMO,LUMO}$ and $2K_{HOMO,LUMO}$.

This effect explains one-third of the change. However, the remaining main part obtained by the CI calculation is yet unknown. Therefore, we have examined the detailed features of the result of CI. The CI coefficient changes as a function of the dihedral angle are shown in Table III and Figure 9. Over all of dihedral angles, a dominant character of the transition is traced by the coefficient of HOMO(63) → LUMO(64) excitation. However, this only slightly decreases, the (56)th → LUMO and the (59)th → LUMO excitation coefficients increase, and, also, the (57)th → LUMO excitation coefficient decreases with the increase of the dihedral angle (18° → 90°). The (56)th and the (59)th orbitals are both characterized as the lone pair belonging to the imino N atom (see Figure 3). The increased mixing of the (56)th → LUMO and the (59)th → LUMO into the HOMO → LUMO excitation signifies the increase of the CI off diagonal matrix element

$$\langle\psi_{HOMO\rightarrow LUMO}|H|\psi_{56\rightarrow LUMO}\rangle$$

and

$$\langle\psi_{HOMO\rightarrow LUMO}|H|\psi_{59\rightarrow LUMO}\rangle$$

When the dihedral angle is small, the HOMO (π-orbital localized and perpendicular in aniline ring) and imino N atom lone pair (the (56)th and the (59)th orbitals, lying in plane of the quinone ring) have a small overlap, namely $\langle\psi_{HOMO\rightarrow LUMO}|H|\psi_{56(or59)\rightarrow LUMO}\rangle$ is small. When the dihedral angle is increased from 18° to 90°, the HOMO and imino N atom lone pair orbital start to overlap virtually, that is $\langle\psi_{HOMO\rightarrow LUMO}|H|\psi_{56(or59)\rightarrow LUMO}\rangle$ increases. Thus the dihedral angle change determines the mixing of HOMO → LUMO excitation and imino N atom lone pair →

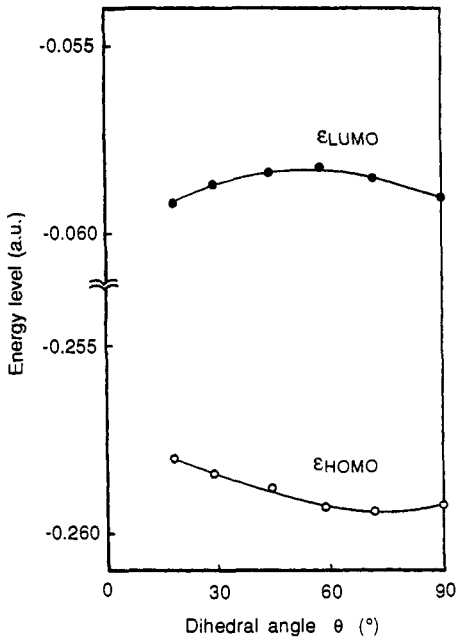

Figure 4. HOMO and LUMO energy levels changes of **2** with changes of the dihedral angle of the quinone and the aniline rings (INDO/S).

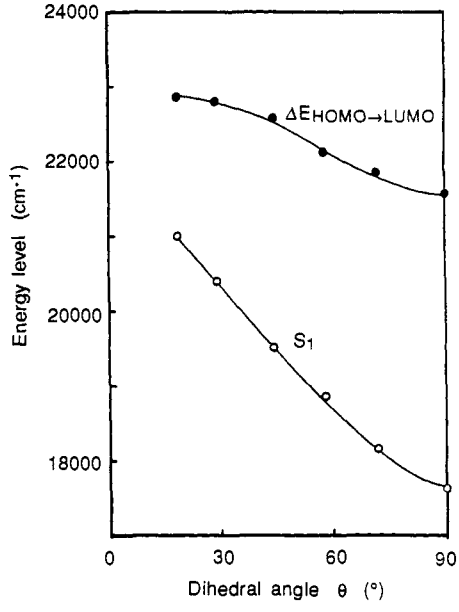

Figure 5. First transition energy level and $\Delta E_{HOMO \rightarrow LUMO}$ changes of **2** with changes of the dihedral angle of the quinone and the aniline rings (INDO/S).

LUMO excitation; the mixing in the imino N atom lone pair leads to a decrease in the transition energy. In other words, the predominately π–π^* CT transition acquires n–π^* character as the dihedral angle increase and this mixing causes the red shift.

As a conclusion of this section, the absorption wavelength change shown in Figure 2 is interpreted by a one-third contribution from the $\Delta E_{HOMO \rightarrow LUMO}$ term and by two-thirds from electron correlation. For the contents of the latter, the intervention of the n–π^* transition into the lowest excited state is characterized.

(iii) The Second Transition (Not Observed, S_2 State). The calculations (Table I) show the near 450-nm transition with almost zero oscillator strength in all dyes. Having almost zero intensity, no observation is expected, and indeed no band near 450 nm appears in Figure 1. However, if the dihedral angle changes, the transition character (and resulting zero intensity) can change. In order to examine this, the change of the second transition as a function of the dihedral angle has been calculated, and the result is shown in Figure 10 for the dye **2**. The transition does not show the dihedral angle dependence; the absorption wavelength of

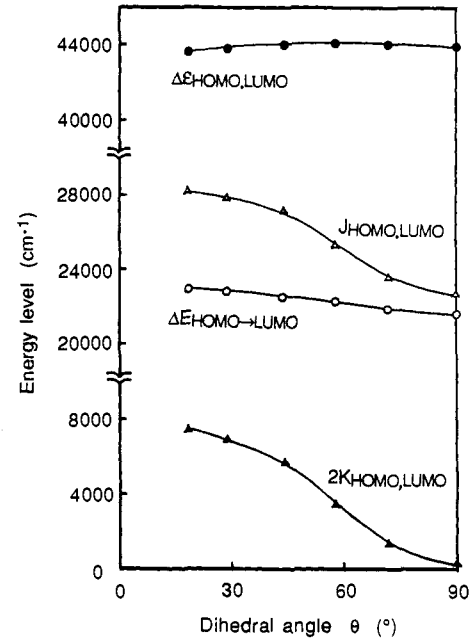

Figure 6. $\Delta E_{HOMO \rightarrow LUMO}$, $\Delta\epsilon_{HOMO,LUMO}$, $J_{HOMO,LUMO}$, and $2K_{HOMO,LUMO}$ changes of **2** with changes of the dihedral angle of the quinone and the aniline rings (INDO/S).

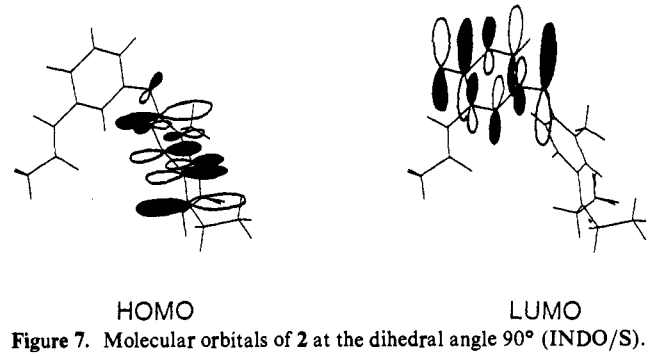

Figure 7. Molecular orbitals of **2** at the dihedral angle 90° (INDO/S).

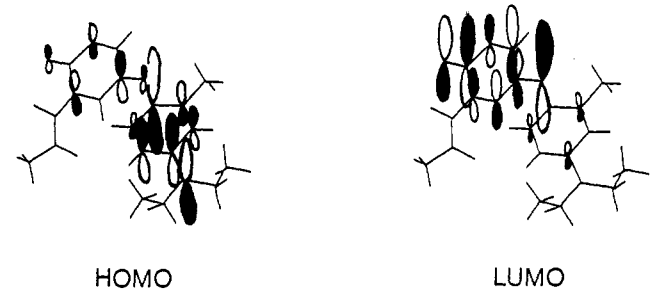

Figure 8. Molecular orbitals of **2** at the dihedral angle 18° (INDO/S).

almost 450 nm and the absorption intensity of almost zero are constantly kept unchanged. The second transition (449 nm) is described by various configurations (Table II). The changes of the CI coefficient with the dihedral angle for important configurations are shown in Figure 11. Although, the CI coefficient changes quite drastically, these excitations are commonly localized on the quinone ring (quinone O atom Py and $NHCOCH_3$ O atom Py orbital → LUMO excitation (see Figure 3)). Owing to the localization within the quinone ring as a whole, the dihedral angle change has no effect on the λ_{max}, and the oscillator strength remains zero, because of the zero overlap of Py orbitals of O atoms and the perpendicular LUMO (z direction).

(iv) The Third Transition (Next Absorption Band, S_3 State). The next observed band (360–370 nm) corresponds to the calculated third transition (Table I). This transition has a high enough extinction coefficient and absorption that tails into the visible region (see Figure 1) such as to be an important influence

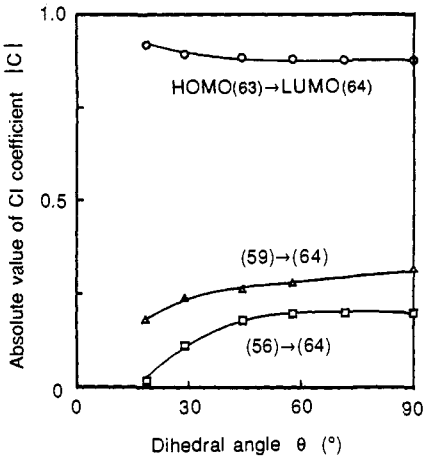

Figure 9. CI coefficient changes of the first transition of **2** with changes of the dihedral angle of the quinone and the aniline rings (INDO/S).

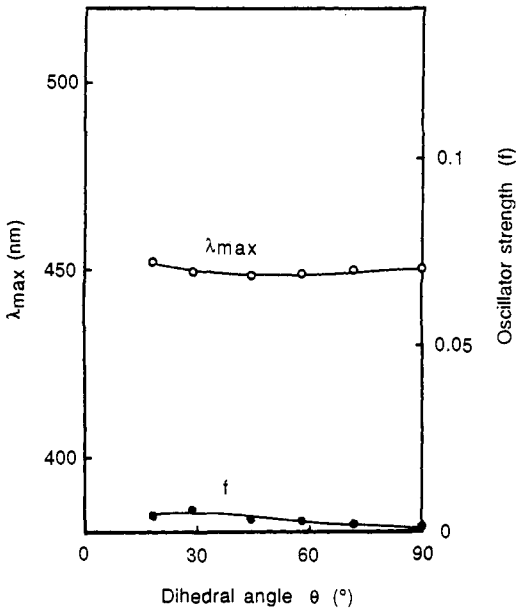

Figure 10. Spectral changes of the second transition of **2** with changes of the dihedral angle of the quinone and the aniline rings (INDO/S).

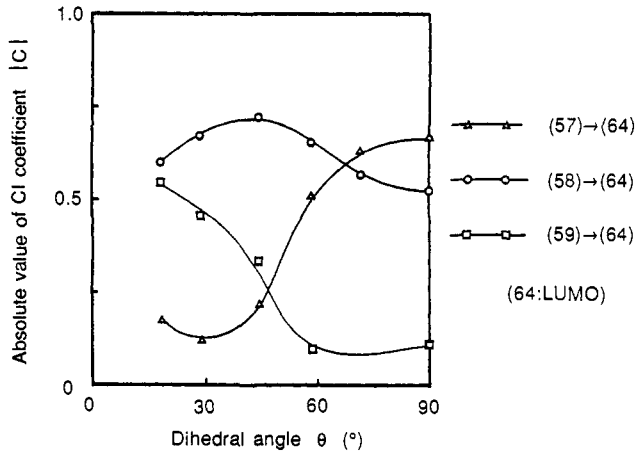

Figure 11. CI coefficient changes of the second transition of **2** with changes of the dihedral angle of the quinone and the aniline rings (INDO/S) (the excitations having the CI coefficient over 0.4 are shown).

on the color of the dye. The change of λ_{max} and oscillator strength with the dihedral angle has been examined for the dye **2** (Figure 12). As the dihedral angle increases, the λ_{max} shows the blue shift and the oscillator strength increases at the beginning (18° → 35°), then slightly decreases later (35° → 60°), and very slightly increases at the vicinity of 90° (60° → 90°). As shown

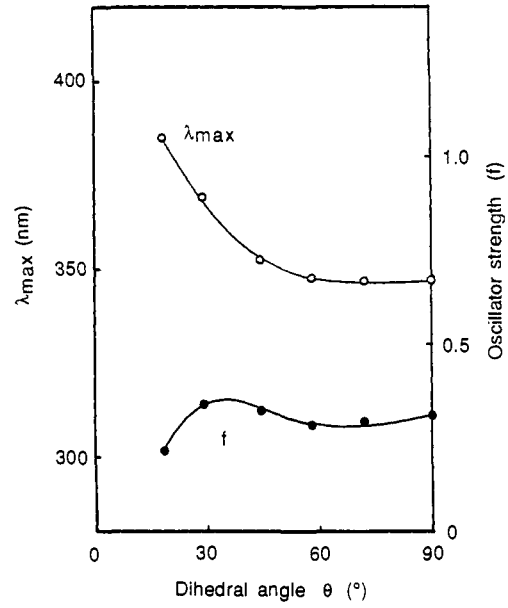

Figure 12. Spectral changes of the third transition of **2** with changes of the dihedral angle of the quinone and the aniline rings (INDO/S).

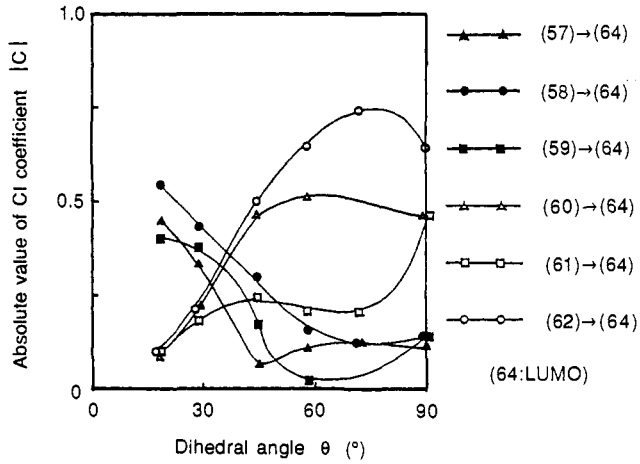

Figure 13. CI coefficient changes of the third transition of **2** with changes of the dihedral angle of the quinone and the aniline rings (INDO/S) (the excitations having the CI coefficient over 0.4 are shown).

in Table II, this transition (353 nm) also consists of various configurations. The CI coefficient changes with the dihedral angle for the important configurations are shown in Figure 13. From Figure 13 and Table II, the important configurations are characterized by the orbitals localized in the quinone ring,[4] with a small weight in the aniline ring.

In the small dihedral angle region (~18°), the main character is assigned as the quinone O atom Py and $NHCOCH_3$ O atom Py orbital → LUMO excitation ((57) → (64), (58) → (64), and (59) → (64)). As the dihedral angle increases (18° → 35°), this character weakens and the π–π^* transition in the quinone ring becomes important ((60 → (64) and (62) → (64)). In the small dihedral angle region, the longer wavelength and the smaller oscillator strength are caused by the O atom Py → LUMO character, since the O atom Py → LUMO excitation originally has low energy and small intensity (see previous section). At dihedral angles larger than 35°, the transition character is relatively unchanged, because this transition is almost entirely from the quinone ring and contributed excitation is almost the same.[21]

B. Substituent Effect (without Including the Steric Effect). In order to examine separately the effect of the dihedral angle and

(21) Although we have examined the dihedral angle of the quinone and the aniline (18–90°), the angle smaller than 35° could be difficult to realize in practice, because of the steric hindrance.

Table IV. Calculated Absorption Spectra of Indoaniline Dyes on the X-ray Structure (Dihedral Angle 44.5° [a]) (INDO/S)

dye	R	R′	λ_{max} (nm)	f [b]
1	H	H	506.0	0.452
			450.3	0.004
			352.1	0.283
2	CH_3	H	512.3	0.467
			448.7	0.003
			352.6	0.324
3	CH_3	CH_3	506.0	0.471
			446.4	0.004
			355.6	0.241
4	$NHCOCH_3$	H	529.0	0.507
			451.1	0.003
			352.7	0.198

[a] X-ray value for dye (**2**). [b] Oscillator strength.

the electronic effect induced by substituents, the calculation at the fixed dihedral angle 44.5° (X-ray value for **2**[18] has been performed for various substituents (Table IV).

For the first transition (Table IV), the substitution by 2′-CH_3 (see **2**) produced a long absorption wavelength and a large oscillator strength compared to unsubstituted **1**. When both hydrogens of 2′- and 6′- are substituted by CH_3 (**3**), again almost the same λ_{max} as unsubstituted (**1**) and the larger oscillator strength than the one substituted (**2**) are obtained. When the substituents with extended π-conjugations such as $NHCOCH_3$ (**4**) are introduced, the longer λ_{max} and the larger oscillator strength are obtained.

The second transition is not considered because it is not observed. The third transition (the next absorption band observed) is not sensitive to the substituents in each molecule, because it is mainly localized on the quinone ring and all the substituents are in the aniline ring.

C. Structure Absorption Relationship and Steric Effect. As shown in Table I, the optimized dihedral angles of **1** and **2** have almost the same value (47°), indicating the similar steric hindrance round the azomethine bridge. Although there is no X-ray data for **1**, the calculated value for **2** reproduces well the X-ray value (44.5°).[18] In 2′, 6′-diCH_3 substituted molecule **3**, the optimized dihedral angle is 68.3°, the largest value among the molecules considered, which is consistent with the large X-ray value of 56.7° for **3**.[18] For the 2′-$NHCOCH_3$ substituted molecule **4**, a smaller dihedral angle (42.0°) than H or CH_3 substituted is apparent owing to the intramolecular hydrogen bond (for details, see the next section).

By comparing Tables I and IV, the steric effects in experimental values are as follows. For the first transition, the relationship between dihedral angle and absorption spectrum in Figure 2 is confirmed. Namely, all the λ_{max} values are larger in Table I (with a larger dihedral angle) relative to the λ_{max} of Table IV (with a fixed value of 44.5°). Specifically, in the molecule **3**, the longest λ_{max} (λ_{max}(obsd) 666 nm, λ_{max}(calcd) 563 nm) and the smallest absorption intensity (ϵ 8400, f 0.116) is obtained for the large dihedral angle of 68.3°. Indeed, molecules having the large bulky substituent around azomethine bridge, such as 2′,6′-disubstituted molecules,[8,11] and 3,5-disubstituted molecules,[3b] have been reported without explanation as having the longer wavelength and the smaller transition probability of absorption. They can now be understood as being caused by the large dihedral angle arising from the bulkiness around the azomethine bridge.

The second transition always shows zero transition probability (Figure 10) and is not observed in any molecule (Figure 1). For the third transition (correspond to the next absorption band observed, Figure 12) contrasting with the first band, no clear structure–absorption relationship appears either in the observation or in the calculation. Therefore in the third transition the dihedral angle dependency (35°–90° region) is not pronounced. However, it should be noticed that the accurate calculation of the second or higher transition is far more difficult than for the first transition.[22,23]

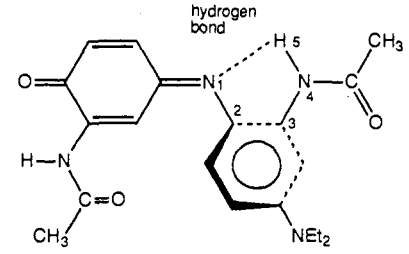

Figure 14. Molecular structure of **4**.

Table V. Absorption Spectra as a Function of Different Magnitude of the Hydrogen Bond in Dye (**4**). Dihedral Angles Fixed (42.0° [a]) (INDO/S)

$\angle C_3N_4H_5$ (deg)	$N_1 \cdots H_5$ (Å)	λ_{max} (nm)	f [b]
90	1.962	531.2	0.548
100	2.098	528.2	0.542
116.0[c]	2.354	524.9	0.536
130	2.595	523.6	0.534
d		493.9	0.477

[a] Optimized by AM1 method for dye (**4**). [b] Oscillator strength. [c] Optimized by AM1 method. [d] $NHCOCH_3$ and aniline ring perpendicular.

D. $NHCOCH_3$ as a Remarkable Substituent. The observed spectrum of the 2′-$NHCOCH_3$ substituted molecule **4** shows very long absorption λ_{max} (622 nm) and the largest extinction coefficient (ϵ 34 100) (Table I). In fact for dye **4**, there is an extra interaction of the intramolecular $N_1 \cdots H_5$ hydrogen bond (see Figure 14). This is suggested by the X-ray structure of the similar molecule.[12f]

First, we have examined the electronic effect of the $NHCOCH_3$ substituent (without including steric effect, i.e., separately from dihedral angle dependency), by using the calculated absorption spectra at the same dihedral angle (44.5°, X-ray value for **2** (Table IV). The **4** shows the longest λ_{max} and the largest oscillator strength in Table IV. In order to consider the hydrogen bond effect on this absorption property, the hydrogen bond length ($N_1 \cdots H_5$) has been artificially modified by bending the $\angle C_3N_4H_5$ angle (see Figure 14) at the fixed dihedral angle (42.0°, optimized value for **4** see Table I). The results are shown in Table V. As the hydrogen bond distance increases (the hydrogen bond being weaken), the λ_{max} becomes shorter, and the oscillator strength decreases. Therefore the intramolecular hydrogen bond plays an important role in causing the electronic effect of long λ_{max} absorption and large absorption coefficient. Moreover, the situation where the $NHCOCH_3$ is perpendicular to the aniline ring is calculated and shown in the last line in Table V. This situation is a model lacking the hydrogen bond with the same substituent. A very short λ_{max} and a very small oscillator strength is obtained. This suggests that the π-conjugation of the NH-$COCH_3$ with the aniline ring is also important for the longer absorption wavelength and the larger intensity.

Secondly the steric effect has been also examined. When the intramolecular hydrogen bond distance is modified, the optimization of a dihedral angle for each distance is carried out, and the calculated absorption spectra are shown in Table VI. As the hydrogen bond distance increases (the hydrogen bond being weakened), the dihedral angle increases. As a result, the λ_{max} has slightly blue shifted and the oscillator strength decreased. When the $NHCOCH_3$ substituent is perpendicular to the aniline ring, the optimized dihedral angle comes to near 47°, and the value is almost the same as H (**1**) or CH_3 (**2**) substituted molecule. This result shows the intramolecular hydrogen bond is responsible for the small dihedral angle.

In conclusion, the long wavelength and the large intensity for dye **4** arise from the electronic effect of $NHCOCH_3$ itself and

(22) (a) Baker, J. D.; Zerner, M. C. *Chem. Phys. Lett.* **1990**, *175*, 192. (b) Baker, J. D.; Zerner, M. C. *J. Phys. Chem.* **1991**, *95*, 8614.
(23) Volosov, A. *J. Chem. Phys.* **1987**, *87*, 6653.

Table VI. Absorption Spectra as a Function of Different Magnitude of the Hydrogen Bond in Dye (4). Dihedral Angles Optimized

$\angle C_3N_4H_5$ (deg)	$N_1 \cdots H_5$ (Å)	dihedral angle[a] (deg)	calcd (INDO/S)	
			λ_{max} (nm)	f[b]
90	1.962	41.2	529.7	0.559
100	2.098	41.6	527.3	0.548
116.0[c]	2.354	42.0	524.9	0.536
130	2.595	42.3	524.2	0.530
d		47.3	498.7	0.410

[a] Optimized by AM1 method. [b] Oscillator strength. [c] Optimized by AM1 method. [d] $NHCOCH_3$ and aniline ring perpendicular.

the intramolecular hydrogen bond (both steric, small dihedral angle, and electronic). The results are consistent with our previous study of naphthoquinone methide dyes.[16]

E. Comparison with Naphthoquinone Methide Dye. Indoaniline dyes and naphthoquinone methide dyes[16] can be compared. The similar behavior of dihedral angle and absorption spectrum relationship has been shown for the first transition band. The absorption spectrum change with a dihedral angle is explained by a CI effect also being related to the imino N lone pair. The similar character is generated by the same type of transition (aniline to quinone CT type transition). However, the detailed features differ in that one-third of the transition energy of indoaniline dyes stems from electronic interaction of HOMO and LUMO orbitals. On the other hand, in naphthoquinone methide dyes, all the transition energy change is reduced to the CI effect.

The second transition of naphthoquinone methide dyes corresponds to neither the second nor the third transition of indoaniline dyes. The origin of the difference in transition character may be explained by the replacement of quinone =O bond by $=C(CN)_2$ in naphthoquinone methide dye, which must strongly influence the second and the third transition in indoaniline dye.

5. Conclusion

On the basis of the results of INDO/S calculations, we have examined the source of the red shift of the first absorption band which is proportional to the increase of dihedral angle. A simple HOMO–LUMO gap explanation was not applicable to this dye. We have found a remarkable configuration interaction to be the reason for the shift. The oscillator strength change is also explained by the change of overlap of the wave functions. This analysis has provided a guiding principle for the design of the indoaniline dyes, as dihedral angle control combined with relevant substituent effect. The next observed absorption band (corresponds to the third transition in the calculation) consists mainly of a quinone ring transition, which depends mainly on the electronic properties of substituents and does not clearly show the dihedral angle dependency.

One of the interesting features of indoaniline dye is that molecules having an azomethine bridge with a steric substituent commonly show the long absorption wavelength and small extinction coefficient of the first absorption band.[3b,8,11] Based on our calculated results, this common behavior is explained by the large dihedral angle caused by the steric hindrance around the azomethine bridge.

The dihedral angle can be controlled by bulkiness, the position of the substituent, or an intramolecular hydrogen bond. Experimental X-ray structures and experimental spectra support this conclusion. The 2′-$NHCOCH_3$ substituent (forming an intramolecular hydrogen bond) in **4** caused a long absorption wavelength shift and large intensity, through both the electronic effect and the hydrogen bond (both electronic and steric) of $NHCOCH_3$.

This study has explained the novel structure–absorption relationship of indoaniline dyes. Indoaniline dyes are only one typical dye among huge number of other dyes. However, the principles developed in the current study (the configuration mixing leading to a red shift) cannot be limited solely to one dye. The example includes our previous study of naphthoquinone methide dyes.[16] Guiding principles for dye design thus obtained may be applicable to a wide range of other dyes that can be nonplanar.

Acknowledgment. The authors thank Professor M. C. Zerner for the INDO/S program.